Simulating thick atmospheric turbulence in the lab with application to orbital angular momentum communication

Brandon Rodenburg,[1] Mohammad Mirhosseini,[1] Mehul Malik,[1] Omar S. Magaña-Loaiza,[1] Michael Yanakas,[1] Laura Maher,[1] Nicholas K. Steinhoff,[2] Glenn A. Tyler,[2] and Robert W. Boyd[1,3]

[1]The Institute of Optics, University of Rochester, Rochester, NY 14627 USA
[2]The Optical Sciences Company, 1341 South Sunkist Street, Anaheim, California 92806
[3]Department of Physics, University of Ottawa, Ottawa ON K1N 6N5 Canada

E-mail: Brandon.Rodenburg@gmail.com

Abstract. We describe a procedure by which a long ($\gtrsim 1\,\mathrm{km}$) optical path through atmospheric turbulence can be experimentally simulated in a controlled fashion and scaled down to distances easily accessible in a laboratory setting. This procedure is then used to simulate a 1-km-long free-space communication link in which information is encoded in orbital angular momentum (OAM) spatial modes. We also demonstrate that standard adaptive optics methods can be used to mitigate many of the effects of thick atmospheric turbulence.

PACS numbers: 42.68.Bz, 42.79.Sz, 03.67.Hk

Submitted to: *New J. Phys.*

1. Introduction

Understanding how light propagates is one of the most fundamental topics in the field of optics. Although this problem is very well understood for deterministic systems, the problem of understanding how light behaves in random or fluctuating media is still a very active area of research [1–4]. Even propagation through the air, which at first glance might be thought of as being equivalent to free-space propagation, will show stochastic behavior when observed over sufficiently long distances due to small random fluctuations in the refractive index along the path.

Early research studying optical propagation along random paths arose in the context of imaging of astronomical objects through the turbulence in atmosphere [5]. The most important effect on image quality in such systems is the random phase imprinted onto the beam by the turbulence. This phase aberration can be described by the quantity r_0, a coherence length scale of the turbulence defined in the receiver aperture and known as Fried's parameter [6,7]. If all other effects of turbulence can be ignored (e.g. amplitude fluctuations), then the turbulence can be approximated by a random phase screen in the aperture of the receiver. This approximation, known as the "thin phase screen approximation," simplifies the problem and allows the turbulence strength to be fully characterized by the dimensionless parameter, D/r_0, where D is the diameter of the aperture or beam. Thus the effects of turbulence depend not only on the intrinsic fluctuations in the air, but also on details of the system. This thin screen approximation is often appropriate in astronomical systems as turbulence effects on beam propagation are greatest where the atmosphere is thickest, which is typically located directly in front of the telescope.

Another area in which understanding the effects of turbulence on optical beams is important is in optical communication in free-space [8]. It is well known that beams of light that contain a phase vortex of the form $\psi(r,\phi) \propto \exp(i\ell\phi)$, where ℓ is an integer, carry orbital angular momentum (OAM). A single photon prepared in such a state will have an OAM equal to $\ell\hbar$ in addition to any angular momentum carried by the polarization [9]. In recent years there has been a good deal of excitement based on encoding information in a free-space channel onto such OAM beams of light [8,10,11], as such modes are a natural basis for such systems (i.e. they are the eigenmodes of a channel with cylindrical symmetry) [12]. Such spatial mode encoding schemes allow for increasing of the bit rate as each pulse may contain more than 2 possible symbols. This scheme also provides an enhancement to the security when used for quantum key distribution [13,14].

Degradation of the signal in a free-space channel due to atmospheric turbulence is a primary limitation to the information-carrying capacity of such a channel. Much work has been done to study how this affects communication systems that utilize spatial mode encoding [15–21]; however much of this work focuses on turbulence that is fully described by a random thin phase screen in the receiver aperture. In more realistic situations, such as communication along a long horizontal path through which the turbulence is

continuously distributed, one will see amplitude fluctuations, that is scintillation, in addition to the problems caused by pure phase fluctuations. Some of this degradation can still be compensated for by phase-only adaptive optics (AO), correcting for low-spatial-frequency aberrations for a horizontal path of a few kilometers or more [22]. For more stronger scintillation one will begin to see intensity nulls that are associated with phase vortices [23, 24]. These phase vortices, or branch points, are known to degrade the performance of AO systems [25], and there is a complete breakdown in the performance for horizontal paths greater than approximately 5 km due to this effect [26]. For communication systems that communicate using OAM, this phenomenon presents an additional problem as phase vortices are precisely the means of the encoding, and randomly generated vortices introduce errors into such a scheme.

The propagation of an optical beam through thick turbulence is not in general analytically solvable and thus requires either simulation or testing in a real world setup. The cost and lack of control of testing in a real-world setup makes finding suitable methods of simulating turbulence highly desirable for understanding this problem. In this paper we describe a method of simulating a thick turbulence channel and show how this can be implemented in a laboratory setup (section 2). To demonstrate the power of this method we simulate a 1-km long free-space OAM-based communication link; these results are presented in section 3.

2. Simulating thick turbulence in the laboratory

To examine the effects that a thick horizontal turbulent path might have on OAM-based communication channel while still allowing information transfer and AO correction, we chose to consider a 1 km path L with aperture sizes of the sender and receiver of $D = 18.2$ cm, at a wavelength of $\lambda = 785$ nm corresponding to a Fresnel number of $N_f = \pi D^2/(4\lambda L) = 33$. The numerical value of N_f is related to the total number of spatial modes that the channel supports, and the value of 33 was chosen to be both realistic as well as large enough to support at least a few dozen OAM modes [12].

To allow for such a system to be realized in a laboratory setting, one must find a way to incorporate turbulence into the channel, as well as properly scale the system down to more manageable length scales. Section 2.1 contains a heuristic description of atmospheric turbulence and its various effects on beam propagation. Section 2.2 describes a method of emulating a thick turbulence path with 2 thin phase screens that can be represented in the lab with spatial light modulators (SLMs). Scaling rules that are invariant under Fresnel propagation are detailed in section 2.3 and the experimental setup is discussed in 2.4.

2.1. Atmospheric turbulence

Turbulence is a phenomenon that occurs in any fluid that is characterized by a large Reynolds number, $\mathcal{R} = V\mathfrak{L}/\nu$, where V is the fluid's mean velocity, $\mathfrak{L}$ is the length

scale of the fluid, and ν is the viscosity. The fluid will then break up into a cascade of turbulent eddies of decreasing size until the length scale, $\mathfrak{L} = l_0$ is such that $\mathcal{R} \leq 1$ and the kinetic energy can be dissipated as heat. l_0 is known as the inner scale and is typically on the order of 1 mm in the atmosphere, negligibly small relative to the length scales in a free-space communication channel [27].

The fluid velocity $v(r)$ at any point r in a turbulent fluid is a random process whose spatial structure can be described by the structure function, defined as $D_v(\mathbf{r_1}, \mathbf{r_2}) \equiv \langle |v(\mathbf{r_1}) - v(\mathbf{r_2})|^2 \rangle$. For $\|\mathbf{r_1} - \mathbf{r_2}\| > l_0$ the structure function is governed by "Kolmogorov statistics," given by

$$D_v = C_v^2 \delta r^{2/3}, \tag{1}$$

where $\delta r \equiv \|\mathbf{r_1} - \mathbf{r_2}\|$, and where C_v^2 is known as the velocity structure parameter which characterizes the strength of the fluctuations [28]. The turbulent eddies will mix the air, creating pockets of slightly different temperatures and thus pressures. As a consequence of this variation in air pressure the index of refraction will also vary statistically in the same way, leading to the refractive index structure function [29]

$$D_n = C_n^2 \delta r^{2/3}. \tag{2}$$

The random fluctuations in the index of refraction is characterized by D_n and lead to a random phase, $\phi(\mathbf{r})$ at the receiver. It was shown by Fried [6] that for Kolmogorov turbulence the phase structure function can be given by

$$D_\phi = 6.88 \left(\frac{\delta r}{r_0} \right)^{5/3}, \tag{3}$$

where r_0 is again Fried's parameter and can be calculated from C_n^2 by the formula

$$r_0 = \left[\frac{2.91}{6.88} k^2 \int_0^L C_n^2(z)\, \mathrm{d}z \right]^{-3/5} = \left[\frac{2.91}{6.88} k^2 C_n^2 L \right]^{-3/5}, \tag{4}$$

where we have assumed for simplicity a constant value for C_n^2 along the path.

A random phase imprinted on an optical beam will, upon propagation, will lead to variations in the amplitude as well, thus modifying the field at the receiver in both the phase and the amplitude. We can write the field as $U(\mathbf{r}) = U_0(\mathbf{r}) \exp\left(i\phi(\mathbf{r}) + \chi(\mathbf{r})\right)$, where U_0 is the field in the absence of turbulence, ϕ is the random phase, and χ is the random log-amplitude. These amplitude fluctuations, or "scintillations" can then be characterized by the variance in χ which is calculated from C_n^2 as [29]

$$\sigma_\chi^2 = 0.563 k^{7/6} \int_0^L C_n^2(z) z^{5/6}\, \mathrm{d}z = \frac{0.563 * 6}{11} k^{7/6} C_n^2 L^{11/6}. \tag{5}$$

Not only does χ cause scintillation within the beam, but this also leads to fluctuations in the total power of the beam, even if there are no losses in the path itself. These power fluctuations are due to beam wander and clipping by the finite

aperture at the receiver. The normalized power over the aperture Σ of area A_Σ, defined by $P \equiv \frac{1}{A_\Sigma} \int_\Sigma \mathrm{d}\mathbf{r} \exp(2\chi(\mathbf{r}))$, is used to numerically find the normalized power variance in the aperture,

$$\sigma_P^2 \equiv \langle P^2 \rangle - \langle P \rangle = \langle P^2 \rangle - 1 = \frac{1}{A_\Sigma^2} \iint_{\Sigma\Sigma'} \left(e^{4C_\chi(\mathbf{r},\mathbf{r}')} - 1 \right) \mathrm{d}\mathbf{r}\,\mathrm{d}\mathbf{r}' - 1, \qquad (6)$$

where $C_\chi(\mathbf{r}, \mathbf{r}') = \langle (\chi(\mathbf{r}) - \langle\chi\rangle)(\chi(\mathbf{r}') - \langle\chi\rangle) \rangle$ is the log-amplitude covariance function [1].

2.2. Two phase screen model

We have found that through use of 2 phase screens we can accurately model the horizontal turbulent channel, faithfully reproducing all of it's relevant statistical properties. Specifically we require this path to have the same values for r_0, σ_χ^2, and σ_P^2 as described in section 2.1.

We can represent these 3 parameters by using thin Kolmogorov phase screens each with its own value of r_0. The values of r_0 for each screen, as well as each screen's position along the path, give us 4 independent parameters that can be tuned until the 2 screen path reproduces the same 3 parameters of the full horizontal channel. This still gives us an additional degree of freedom, and since phase vortices in ϕ create significant problems for AO correction as well as for OAM based encoding [23–26], we choose the density of branch points, ρ_{BP}, as our fourth parameter to constrain the problem.
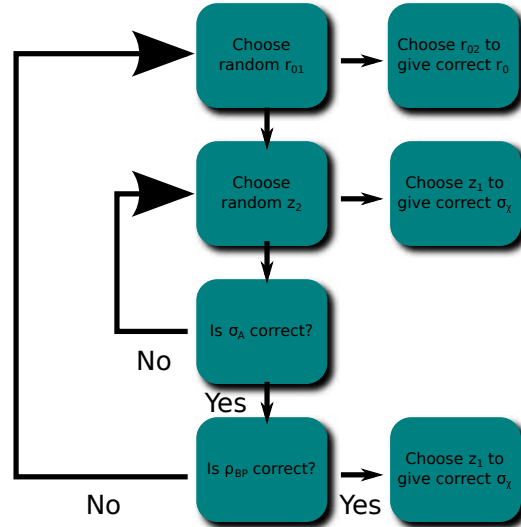

Figure 1. Procedure used to compute Fried's parameters and positions of the two thin phase screens needed to reproduce r_0, σ_χ, σ_p, and ρ_{bp} of the equivalent thick channel.

For a horizontal path with a constant value of the refractive index structure parameter $C_n^2 = 1.8 \times 10^{-14}\,\mathrm{m}^{-2/3}$, which represents a typical horizontal path near ground level, we compute the parameters given in Eqs. 4-6. The computed values are $r_0 = 24.4\,\mathrm{mm}$, $\sigma_\chi^2 = 0.197$, and $\sigma_P^2 = 7.04 \times 10^{-3}$. By Monte-Carlo simulation the density

of branch points in ϕ is found to be $\rho_{BP} = 500/\text{m}^2$. Physically this means that a typical realization of turbulence will create 13 phase vortices within the receiver's aperture, which one could imagine being a serious impediment to one's ability to measure the intended phase vortex of the original transmitted OAM state.

The second step in designing the two-phase-screen model is to find the values for the position and r_0 for each screen that will give the same values of r_0, σ_χ, σ_p, and ρ_{bp} of the thick path. The procedure is diagrammed in Fig. 1. One starts with an initial guess for r_{01} (i.e. r_0 for screen one), and then solves for the value of r_{02} that will give the correct value for D/r_0. Next, one randomly picks a value for the position of the second screen, z_2, and finds z_1 such that one gets the correct value for σ_χ. z_2 is then varied (along with z_1 to maintain σ_χ) to set the correct value for σ_P. Given this solution, ρ_{BP} is computed by Monte-Carlo simulation. If at this point we get the correct ρ_{BP}, a solution has been found; otherwise one starts over with a new choice for r_{01}. Using this procedure we found we could simulate our 1 km path with the parameters $r_{01} = 3.926\,\text{cm}$, $r_{02} = 3.503\,\text{cm}$, $z_1 = 171.7\,\text{m}$ and $z_2 = 1.538\,\text{m}$ (measured from the sender's aperture).
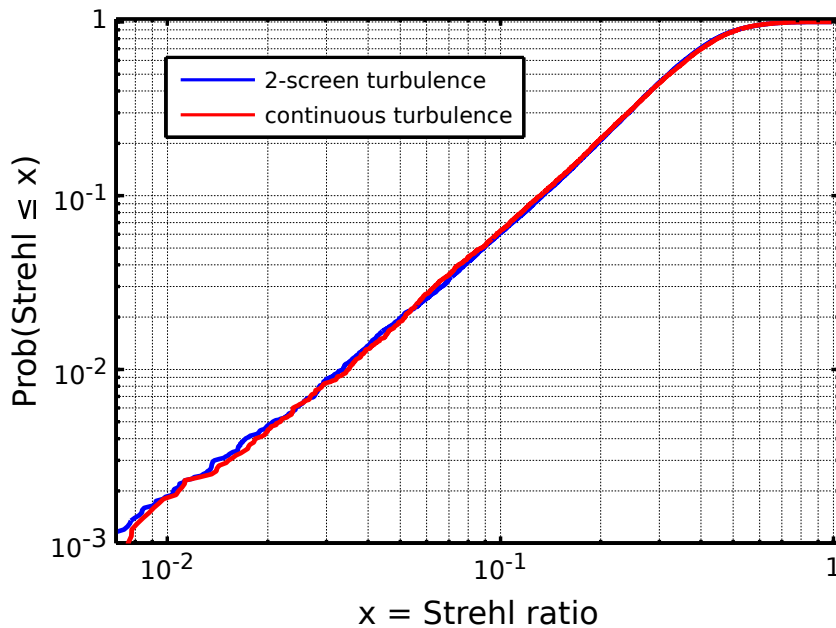
Figure 2. Cumulative distribution function (CDF) of the Strehl ratio for a thick turbulent path represented by 10 Kolmogorov phase screens (red line) and its equivalent 2 phase screen solution (blue line).

As an independent test of this solution, a beam propagation simulation was performed to compare a thick turbulent path with the analogous 2-screen solution. The continuous path was simulated using a standard split-step method in which the path L is broken up into N discrete steps. Each of the N sections of turbulent atmosphere is replaced by non-turbulent propagation followed by an effective thin random phase screen that represents the effects of refractive index fluctuations within the slab. The propagation through a slab can be approximated by a thin screen so long as the

scintillation due to propagation after encountering a random phase is negligible. As a rule of thumb one must require that the scintillation due to propagation through the slab must be less than 10% of the total amount [30] in order to be able to represent the slab by a single screen, which is quantified as

$$\sigma_\chi^2(L/N) < 0.1\sigma_\chi^2(L). \tag{7}$$

We choose $N = 10$, which for the horizontal path considered here becomes by Eq. 5

$$\sigma_\chi^2(L/N)/\sigma_\chi^2 = N^{-11/6} \approx 0.01 \ll 0.1. \tag{8}$$

In each simulation a different random realization of turbulence was made and the Strehl ratio, defined as the ratio of the peak intensity to ideal peak intensity of a spot at a focal plane of the receiver, was computed. By repeating this many times, a probability distribution for the Strehl ratio was found and the results are shown in Fig. 2. As can be seen in the plot, the Strehl ratios of the 2 screen and the 'continuous,' 10 screen paths show very good agreement with each other. This result demonstrates that the 2 screen model not only reproduces the correct mean values for the statistical parameters of interest (by construction), but can also be expected to give similar distributions of possible measurement outcomes.

2.3. Fresnel scaling

The second thing that must be done to effectively simulate a turbulent path in a laboratory setting is to scale the optical paths down to more manageable lengths. In order to ensure that the scaled path still represents the desired physical path, the propagation must remain invariant under the scaling. Fresnel propagation from one
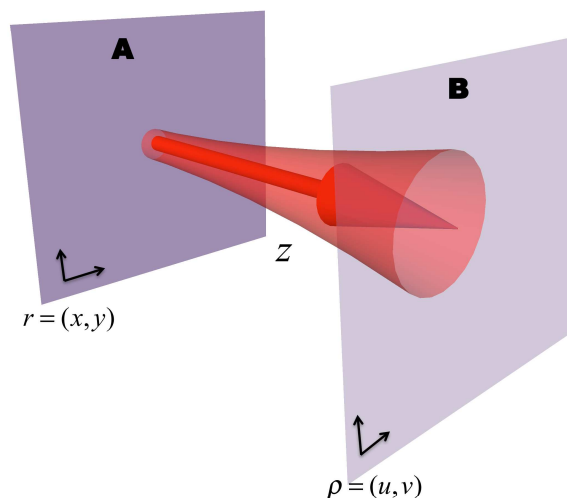
Figure 3. Propagation from plane A, described by coordinates $r = (x, y)$, to plane B with coordinates $\rho = (u, v)$

plane to another a distance z away as shown in Fig. 3 is given by:

$$U_B(\rho) = \frac{ie^{ikz}}{\lambda z} \int U_A(r) e^{\frac{i\pi}{\lambda z}(r-\rho)^2} \, d^2r \qquad (9)$$

Now if we scale the coordinates using $r' = \alpha_r r$, $\rho' = \alpha_\rho \rho$, and $z' = \alpha_z z$ then the above propagation equation becomes:

$$U_B\left(\frac{\rho'}{\alpha_\rho}\right) = \frac{ie^{ikz'/\alpha_z}}{\alpha_r \lambda z'/\alpha_z} \int U_A\left(\frac{r'}{\alpha_r}\right) e^{\frac{i\pi\alpha_z}{\lambda z'}\left(\frac{r'}{\alpha_r} - \frac{\rho'}{\alpha_\rho}\right)^2} \, d^2r' \qquad (10)$$

Since we require the Fresnel number to remain constant, $\alpha_z = \alpha_\rho \alpha_r$. Then we can rewrite equation 10 as:

$$\frac{e^{ikz'(1-1/\alpha_z)}}{\alpha_\rho} U_B\left(\frac{\rho'}{\alpha_\rho}\right) = e^{-i\frac{\pi\rho'^2}{\lambda f_\rho}} \left(\frac{ie^{ikz'}}{\lambda z'} \int U_A\left(\frac{r'}{\alpha_r}\right) e^{-i\frac{\pi r'^2}{\lambda f_r}} e^{\frac{i\pi}{\lambda z'}(r'-\rho')^2} \, d^2r'\right) \qquad (11)$$

where $f_\rho = z'/\left(1 - \frac{\alpha_r}{\alpha_\rho}\right)$ and $f_r = z'/\left(1 - \frac{\alpha_\rho}{\alpha_r}\right)$. From Eq. 11 we see that the horizontal path between planes A and B can be scaled down (to within a scaling and phase constant) simply by adding a lens with focal length f_r at A, propagating a distance z', and then adding another lens with focal length f_ρ at B to cancel out the residual quadratic phase.

2.4. Experimental setup
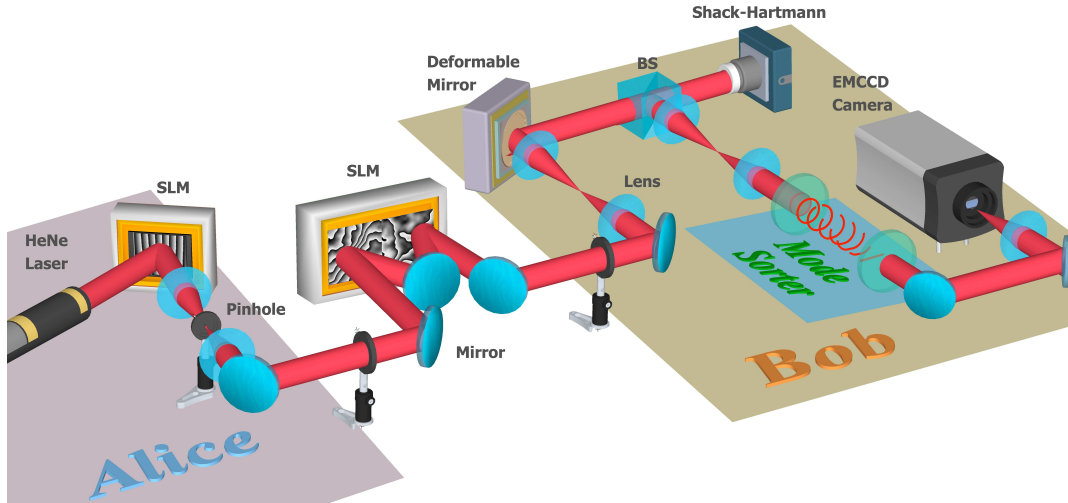
Figure 4. Alice sends a beam prepared in a specific OAM state, ℓ, to Bob. Bob receives the beam after propagation through a channel representing a 1 km turbulence path. The beam is (optionally) corrected using a deformable mirror and sent to a sorter to make a measurement of the of the OAM spectrum of the beam.

A diagram of our experimental setup is presented in Fig. 4. The sender, Alice, prepares a beam in a specific OAM state to send to the receiver, Bob, from an attenuated

HeNe using a spatial light modulator (SLM) combined with a $4f$ system. Diffraction gratings with spatially modulated properties can be shown to create any complex spatial field distribution in the first diffracted order (selected by the $4f$ filter) [31]. This applies whether the grating is an amplitude [32,33] or phase [34] only hologram. A phase-only SLM was used in our experiment to allow for maximum efficiency in generating the modes. The prepared state is then sent through the simulated 1 km path scaled down as described in section 2.3 to a total length of 1.3 m. The two thin phase screens used to simulate thick turbulence in our setup (section 2.2) were implemented using an SLM in a double-pass configuration. In addition, the quadratic phases required for proper scaling of the propagation path were added to the phases on the SLMs.

After propagation through the turbulent channel, the beam at Bob's aperture is imaged with a $4f$ system onto a Thorlabs adaptive optics (AO) kit consisting of a 12×12 actuator deformable mirror and a Shack-Hartmann wavefront sensor. After the AO system, the beam is similarly imaged onto the first element (R1) of the OAM sorter. The OAM sorter uses two refractive optical elements (R1 and R2) and a Fourier transforming lens (FT Lens) to spatially separate different OAM modes allowing for the OAM spectrum to be efficiently measured as described in [35].

3. Experimental results

In order to examine the effects of the turbulent channel on OAM communication, we experimentally measured the OAM spectrum that Bob detects conditioned on what Alice sent. In a perfect channel, if Alice sends OAM mode s, then Bob will measure an OAM spectrum that is simply a Kronecker delta centered at the same mode. However, in an imperfect or turbulent channel, there will be some spreading into neighboring OAM modes to the prepared state. The conditional probability matrix, $P(d|s)$ where d is the detected OAM mode and s is the sent mode, provides a natural expression for this crosstalk induced by the imperfections or turbulence in the channel.
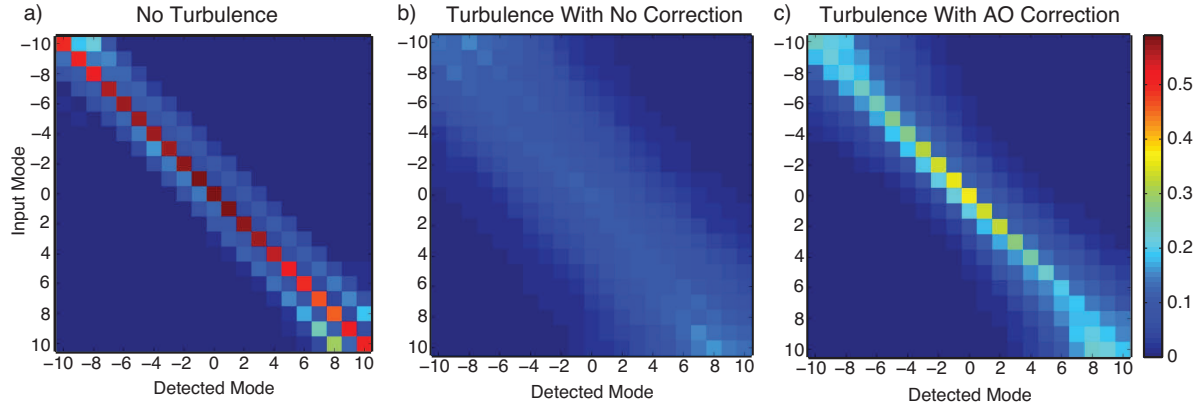
Figure 5. Measurement of the crosstalk in the channel represented by the conditional probability matrix, $P(d|s)$ for three cases: a) no turbulence, b) with turbulence, and c) with turbulence and adaptive correction.

$P(d|s)$ is plotted for 3 different scenarios in Fig. 5. Fig. 5a shows $P(d|s)$ when there is no turbulence in the channel, showing only crosstalk due to any misalignment in the system and inherent crosstalk of the sorter [35]. Fig. 5b shows the effects of thick turbulence ensemble averaged over 100 realizations, which act to greatly spread the signal over many neighboring channels. This selective spreading of OAM into neighboring modes rather than randomly into any OAM state is qualitatively similar to what is seen in the thin turbulence regime demonstrated in [17]. For the third case shown in Fig. 5c, adaptive correction was applied to the turbulence with the AO system, allowing much of the signal to be recovered. The phase aberrations induced from each realization of turbulence was sensed and corrected by the AO using the OAM $\ell = 0$ mode. Each mode was then sent through the channel and AO system, and the OAM spectrum was measured by Bob. This procedure was repeated and averaged over 50 realizations of turbulence.
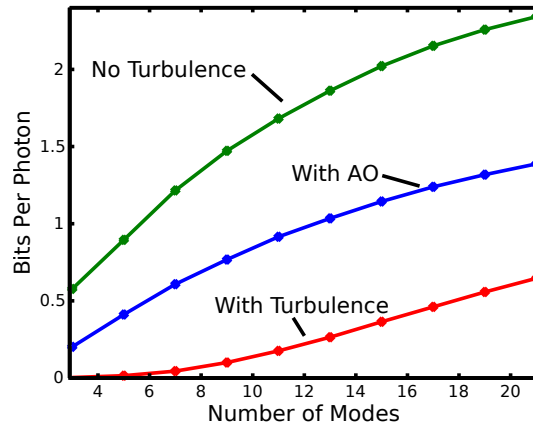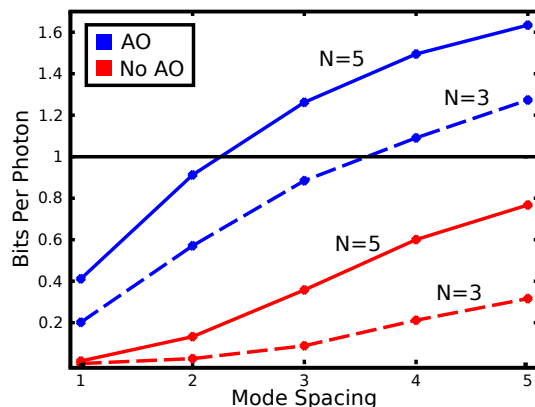

Figure 6. Measured channel capacity as a function of the number of OAM modes used for the spatial encoding.

In order to quantify the crosstalk induced by the turbulence as well as the quality of the AO correction, we compute the mutual information between Alice and Bob for all three cases above. The mutual information between Alice and Bob, $I(A; B)$, provides a measure of the channel capacity, as it gives the maximum possible transmission rate that can be extracted by Bob in bits per photon (or classically per detected pulse). The mutual information is given by the expression,

$$I(A; B) = \frac{1}{N} \sum_{s,d} P(d|s) \log_2 \left(\frac{P(d|s)N}{\sum_s P(d|s)} \right),$$ (12)

where N is the number of distinct symbols. Fig. 5 qualitatively shows that thick turbulence greatly degrades the quality of the channel. Using Equation 12, we quantify these results by calculating the mutual information as a function of the encoding dimension N. The mutual information for the three cases of no turbulence, thick turbulence, and turbulence with AO correction, is plotted in Fig. 6 as a function of

N. One can see that the AO system allows us to cancel roughly half of the loss of channel capacity due to turbulence.

Figure 7. Measured channel capacity as a function of the spacing between OAM modes used for communication.

Further, since turbulence preferentially scatters power into neighboring OAM modes rather than randomly into all modes, one can increase the channel capacity by choosing to use a less dense set of OAM modes [19]. For instance, rather than encoding every OAM mode, one can encode in every second mode (or third or fourth mode etc.). Changing the encoding is also independent of any AO system one may use, and thus a modified encoding can be used along with AO correction to further enhance the channel capacity. Fig. 7 shows the increase in the mutual information one can obtain for a given number of encoded modes, N. The channel capacity of an ideal 2-bit system is shown for reference. It is worth noting that the use of spatial mode encoding shows an improvement over such a system with very moderate resources (i.e. 3 modes with a channel spacing > 4).

4. Conclusions

In this work we have demonstrated how one can experimentally simulate a thick horizontal turbulent path as part of a free-space communication channel. This model was applied to the case of a 1 km path and the effects were studied in the context of an OAM communications channel. It was shown that although the turbulence severely degraded the channel, a high information capacity was still possible by optimizing the encoding and adaptively correcting for some of the induced phase aberrations.

References

[1] Andrews L C and Phillips R L 2005 *Laser Beam Propagation through Random Media* 2nd ed. Press Monographs (SPIE Press)

[2] Popoff S M, Lerosey G, Carminati R, Fink M, Boccara A C and Gigan S 2010 *Phys. Rev. Lett.* **104** 100601

[3] Vellekoop I M, Lagendijk A and Mosk A P 2010 *Nat. Photonics* **4** 320–322

[4] Metzger J J, Fleischmann R and Geisel T 2013 *Phys. Rev. Lett.* **111** 013901

[5] Young A T 1974 *The Astrophysical Journal* **189** 587

[6] Fried D L 1965 *J. Opt. Soc. Am.* **55** 1427

[7] Fried D L 1968 *J. Opt. Soc. Am.* **58** 961

[8] Wang J, Yang J Y, Fazal I M, Ahmed N, Yan Y, Huang H, Ren Y, Yue Y, Dolinar S, Tur M and Wilner A E 2012 *Nat. Photonics* **6** 488–496

[9] Allen L, Beijersbergen M, Spreeuw R and Woerdman J P 1992 *Phys. Rev. A* **45** 8185–8189

[10] Gibson G, Courtial J, Padgett M J, Vasnetsov M, Pas'ko V, Barnett S M and Franke-Arnold S 2004 *Opt. Express* **12** 5448

[11] Boyd R W, Jha A, Malik M, O'Sullivan C, Rodenburg B and Gauthier D J 2011 *Proceedings of SPIE* **7948** 79480L–6

[12] Mirhosseini M, Rodenburg B, Malik M and Boyd R W 2013 *Journal of Modern Optics* pp. 1–6 `1304.0709`

[13] Bourennane M, Karlsson A, Björk G, Gisin N and Cerf N 2002 *J. Phys. A: Math. Gen.* **35** 10065–10076

[14] Cerf N, Bourennane M, Karlsson A and Gisin N 2002 *Phys. Rev. Lett.* **88**

[15] Paterson C 2005 *Phys. Rev. Lett.* **94**

[16] Tyler G A and Boyd R W 2009 *Opt. Lett.* **34** 142

[17] Rodenburg B, Lavery M P J, Malik M, OSullivan M N, Mirhosseini M, Robertson D J, Padgett M J and Boyd R W 2012 *Opt. Lett.* **37** 3735

[18] Gbur G and Tyson R K 2008 *J. Opt. Soc. Am. A* **25** 225

[19] Malik M, O'Sullivan M N, Rodenburg B, Mirhosseini M, Leach J, Lavery M P J, Padgett M J and Boyd R W 2012 *Opt. Express* **20** 13195 `1204.5781`

[20] Roux F 2011 *Phys. Rev. A* **83**

[21] Boyd R W, Rodenburg B, Mirhosseini M and Barnett S M 2011 *Opt. Express* **19** 18310

[22] Levine B M, Martinsen E A, Wirth A, Jankevics A, Toledo-Quinones M, Landers F and Bruno T L 1998 *Applied Opt.* **37** 4553

[23] Fried D L and Vaughn J L 1992 *Applied Opt.* **31** 2865

[24] Tyler G A 2000 *J. Opt. Soc. Am. A* **17** 1828

[25] Fried D L 1998 *J. Opt. Soc. Am. A* **15** 2759

[26] Primmerman C A, Price T R, Humphreys R A, Zollars B G, Barclay H T and Herrmann J 1995 *Applied Opt.* **34** 2081

[27] Quirrenbach A 2006 *A. Extrasolar planets. Saas-Fee Advanced Course* **31** 129–144

[28] Kolmogorov A 1961 *Turbulence: Classic Papers on Statistical Theory* (edited by S K Friedlander and L Topper) s.k. fried ed. pp. 151–155 (Wiley-Interscience)

[29] Tatarski V I 1961 *Wave Propogation in a Turbulent Medium* (McGraw-Hill Books)

[30] Martin J M and Flatté S M 1988 *Applied Opt.* **27** 2111–2126

[31] Arrizón V, Ruiz U, Carrada R and González L A 2007 *J. Opt. Soc. Am. A* **24** 3500

[32] Mirhosseini M, Magaña Loaiza O S, Chen C, Rodenburg B, Malik M and Boyd R W 2013 *Opt. Express* **21** 30196

[33] Rodenburg B, Mirhosseini M, Magaña Loaiza O S and Boyd R W 2014 *arXiv:1312.6878* `1312.6878`

[34] Gruneisen M T, Miller W A, Dymale R C and Sweiti A M 2008 *Applied Opt.* **47** A32

[35] Lavery M P J, Robertson D J, Berkhout G, Love G D, Padgett M J and Courtial J 2012 *Opt. Express* **20** 2110